NPL
National Physical Laboratory

Report

NPL REPORT
DQL-AC 016

Transient response of the IEC 60318-1 artificial ear

Triantafillos Koukoulas and Richard Barham

NOT RESTRICTED

SEPTEMBER 2006

dti
FUNDED BY THE DTI

National Physical Laboratory | Hampton Road | Teddington | Middlesex | United Kingdom | TW11 0LW

Switchboard 020 8977 3222 | **NPL Helpline** 020 8943 6880 | **Fax** 020 8943 6458 | **www.npl.co.uk**

Transient response of the IEC 60318-1 artificial ear

Triantafillos Koukoulas and Richard Barham
Quality of Life Division, Acoustics

ABSTRACT

The calibration requirements for objective audiometry differ from techniques that have been established for traditional hearing testing with pure tones, in that a short duration stimulus is used typically. A calibration based on an impulse response of the ear simulator is therefore considered to be more appropriate than a steady-state response. A method of measuring the impulse response to a volume velocity input has been developed based on transforming the wideband steady-state frequency response using the inverse Fourier transform. This was adapted from a new technique for measuring the acoustical impedance of the ear simulator that has been developed separately at NPL. Calibration results of the impulse response of the IEC 60318-1 artificial ear have been obtained. Current IEC recommended practice is to characterise the transient response of the artificial ear by its steady-state response at 1 kHz. Results obtained for the impulse response have therefore been compared with the response at 1 kHz and differences in sensitivity of 14 dB have been demonstrated. This report then makes a series of recommendations on how the calibration process and IEC recommendations should be changed, with potentially significant disruption to current practices.

ISSN 1744-0599

National Physical Laboratory
Hampton Road, Teddington, Middlesex, TW11 0LW

Approved on behalf of the Managing Director, NPL
by Dr Martyn Sené, Director, Quality of Life Division

CONTENTS

1. INTRODUCTION

Pure tone audiometry has been the cornerstone of hearing assessment for many decades. However, objective methods are now used for widespread screening and in applications where a subjective response is not possible. Often these methods utilise short-duration acoustic stimuli to elicit the objective response. Examples of such applications include otoacoustic emission, where an involuntary acoustic response can be transmitted back through the hearing mechanism, or evoked response audiometry, which uses electric potential measurements (EEG) on the head to identify activity from the auditory nerve. A short duration stimulus is needed in such applications to enable discrimination of the evoked response in time, for example to enable correlation of this response with the input stimulus, or to determine latency in the received signal.

As these methods become incorporated into the overall hearing assessment strategy in the UK, for example through the Universal Neonatal Hearing Screening Programme (http://www.nhsp.info), it is important to consider whether alternative approaches to calibration need to be developed, particularly of the ear simulators that underpin calibration and traceability for such measurements.

This report considers the issue of whether the well-established technique for steady-state calibration is still applicable when the acoustic stimulus applied is one of short or limited duration.

The objectives of this research are therefore:

- To develop a method of determining the sensitivity of ear simulators to transient stimuli, enabling a comparison with the steady-state response to be made

- To consider the impact of any differences between transient and steady-state responses on the current practise recommendations in international standards

- To lay the foundation for a calibration method suitable for applications employing short – duration stimuli.

This report is a deliverable for Project 1.4.4, “Traceability for Objective audiometry” of the NMS Acoustics Programme 2004-2007 of the Department of Trade and Industry.

2. BACKGROUND

The calibration of audiometers and other instrumentation used in the assessment of hearing, and in particular the transducers used to deliver the acoustic stimulus, is underpinned by measurements utilising ear simulators[1]. Ear simulators are devices that enable the acoustic output of a transducer to be measured objectively, while providing an acoustic load that approximates that of a nominal human (adult) ear. There are many types of commercial ear simulators, each being designed to suit a particular class of earphone and the variety of configurations used to couple them to the ear. Ear simulators are available that simulate either the whole outer ear or the occluded ear canal, down to the eardrum. One example of each is considered within this report. Both are standardised by the International Electrotechnical Commission, IEC. The first, known as the artificial ear is standardised in IEC 60318-1[2] and the second, known as the occluded ear simulator, is covered by IEC 60711[3], which will be re-numbered as IEC 60318-4 on revision.

Ear simulators contain a measurement microphone to measure the sound pressure generated within the device. The usual task of calibrating the ear simulator then involves the pressure calibration of this microphone, in isolation from the remainder of the ear simulator.

This is acceptable under steady-state conditions, for example when the transducer to be measured is driven sinusoidally. However in applications utilising short duration signals, it is also necessary to take account of the propagation of the stimulus though the ear simulator elements that couple the source transducer to the microphone.

Some consideration needs to be given to the parameters that need to be measured in order to characterise the ear simulator from the location of the source, through to the microphone output. Furthermore it is necessary to depart from traditional steady-state measures and consider the response to short duration acoustic inputs in the time domain, utilising the *impulse response* of the system. Section 4 describes an experimental method for measuring the impulse response and develops these ideas further.

Using the impulse response of an ear simulator as the basis for calibration, for applications utilising short duration acoustic stimuli, is a new approach developed by NPL that needs to be placed in context with existing IEC recommended practices. IEC 60645-3 currently recommends a protocol for calibration by specifying reference stimuli and methods for measuring and specifying their level[4]. It is not the intention that these signals necessarily be used for actual hearing assessment practice. They merely provide a reference to enable measurement systems to be set up and calibrated on a common basis. The Standard recommends two types of reference electrical inputs; a rectangular pulse of specified magnitude and duration, and a tone burst with defined rise, sustain and fall periods.

The transducer will potentially distort these idealised signals (very likely in the first case), but the standard recommends the determination of the steady-state response resulting in the equivalent peak-to-peak pressure indicated by the system, as the basis for calibration. In the case of the rectangular pulse where there is no intrinsic frequency input, a frequency of 1 kHz is specified for obtaining this equivalent

response. The implicit assumption here is that the transient response of the ear simulator is the same as the steady-state response. One objective of this research is to examine this assumption.

This work focuses on the artificial ear to develop a calibration method based on the impulse response. The rationale is that the principles underpinning the method can readily be transferred to the calibration of the occluded ear simulator in the future, addressing the specific issues associated with that device.

3. CONSIDERATIONS FOR OBTAINING THE IMPULSE RESPONSE

As highlighted previously, the steady-state pressure response of an ear simulator is simply characterised by the response of its measurement microphone, but in the case of the impulse response, account also needs to be taken of the coupling impedance provided by the ear simulator. This raises the question about what input quantity should be considered if the sound pressure is inappropriate. Sound sources (e.g. earphones) are characterised not by the sound pressure they produce (as this depends on the space they transmit into), but by their volume velocity. The acoustical impedance coupling the earphone to the microphone then determines the sound pressure developed and ultimately, together with the microphone sensitivity, the output voltage from the ear simulator. It is sensible therefore to consider the response of the ear simulator to a volume velocity input, and to define the volume velocity sensitivity, L, of the device, as the ratio of output voltage to the applied volume velocity.

By considering a sound source of volume velocity u_1, coupled through an acoustical impedance Z_a, to a measurement microphone having a pressure sensitivity M_2, it follows directly from the definitions of these parameters that the volume velocity sensitivity is simply given by,

$$L = Z_a M_2 \qquad [1]$$

Given that the microphone sensitivity M_2 is readily available from a number of established calibration methods, the task becomes one of determining the acoustical impedance of the ear simulator and of evaluating the impulse response.

A number of methods exist for determining directly the impulse response of dynamic systems, using impulsive stimuli. However these become difficult with small acoustic transducers of limited bandwidth, sensitivity and linearity. A better approach is to use the transformations between the frequency and time domains facilitated by the Fourier transform and its inverse where,

$$\text{Impulse Response} = \text{FFT}^{-1}\ (\text{Frequency Response})$$

Details of implementing this relationship are considered in Section 5. However the implication is that the work can first focus on a method of measuring the acoustical impedance as a function of frequency, to enable the volume velocity frequency response to be determined, and then applied in the above transform to yield the impulse response.

4. MEASUREMENT OF THE ACOUSTICAL IMPEDANCE

The measurement of the acoustical impedance of the artificial ear has been considered recently with the revision of IEC 60318-1 and has been the subject of EUROMET Project 791, "Measurement of the acoustical impedance of artificial ears".

The proposed method being considered in the EUROMET project derives from reciprocity calibration of measurement microphones[5]. In reciprocity calibration, the sensitivity product of two microphones coupled by a known impedance, can be determined by using one microphone as a transmitter to provide an acoustic stimulus, while detecting the resulting sound pressure with the second microphone. The sensitivity product is derived from the ratio of the electrical transfer impedance between the terminals of the microphones, to the acoustical transfer impedance of the acoustic coupling element,

$$M_1 M_2 = \frac{V_0}{i} \frac{1}{Z_a} \qquad [2]$$

where M_1 and M_2 are the respective pressure sensitivities of the transmitter and receiver microphones, i is the electrical current driving the transmitter microphone, V_0 is the open-circuit output voltage from the receiver microphone, and Z_a is the coupling acoustical impedance.

Individual microphone sensitivities are then obtained by introducing a third microphone into the scheme, leading to three possible pair wire combination.

Adapting this approach, it becomes feasible to couple two *calibrated* microphones with a coupling element of *unknown* acoustic transfer impedance. A point to note is that in the formal derivation of Eq. 2, V_0 denotes the open-circuit output voltage of the microphone in order to evaluate the sensitivity of the microphone under idealised electrical load conditions. However, it is equally valid to consider the output from the microphone under a specific electrical load, or indeed from a microphone system, following some signal conditioning or amplification stage (e.g. the preamplifier normally used with a microphone). This approach is valid provided that M_2 is the sensitivity of the microphone or microphone system determined under the same conditions. To avoid confusion, this output voltage will be denoted by V_2. So re-arranging Eq. 2, the acoustical transfer impedance can be determined from,

$$Z_a = \frac{V_2}{i} \frac{1}{M_1 M_2} \qquad [3]$$

In reciprocity calibration, the electrical current applied to the transmitter is normally determined by measuring the voltage across a known impedance placed in series with the microphone. Furthermore, a capacitor is sometimes used for practical convenience.

If this capacitor has capacitance *C* then,

$$Z_a = \frac{V_2}{V_1}\frac{1}{j\omega C}\frac{1}{M_1 M_2} \qquad [4]$$

where ω is the angular frequency and V_1 is the voltage across the capacitor.

Substituting this acoustical impedance in Eq. 1 leads to the expression for the volume velocity sensitivity,

$$L = \frac{V_2}{V_1}\frac{1}{j\omega C}\frac{1}{M_1} \qquad [5]$$

Implementation of Eq. 5 then provides the basis for the experimental system illustrated in Fig. 1.

In this system the transmitter microphone is an IEC type WS2P. It is connected to a purpose-built transmitter adapter through which the transmitter current is applied. This adapter has the correct geometrical configuration for the electrical terminals to which the microphone is connected. This is vital if the microphone is to preserve its calibrated sensitivity. The polarising voltage required by the microphone is also applied using this adapter.

The transmitter microphone is housed flush in a round plate, without its protective grid fitted. This plate contained a circular recess to enable it to be located and coupled to the ear simulator. A photograph of the coupled arrangement can be seen in Fig. 2.

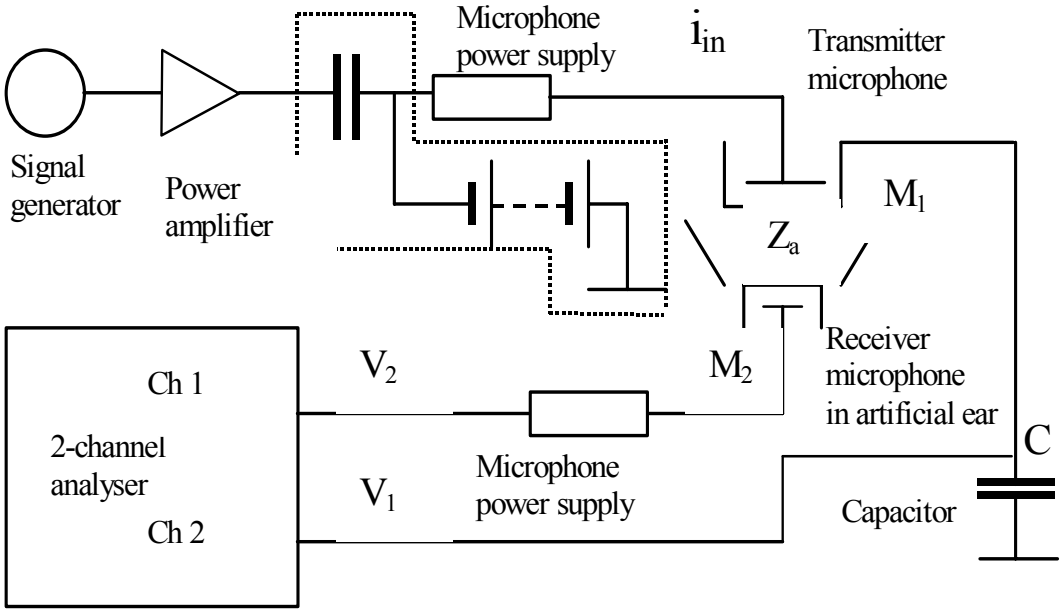

Figure 1. Schematic diagram of measurement system

The capacitor used to measure the input current had a nominal value of 4.7 nF. This was chosen to maintain V_1 and V_2 at approximately equal levels as far as possible, thus reducing the demands on the linearity of the 2-channel analyser.

The system was operated in stepped-sine mode, where the frequency of the signal generator was linked to, and controlled by, the analyser. This enabled the voltage ratio to be measured under steady-state conditions with a prescribed accuracy before moving to the next frequency.

A full list of equipment used can be found in Appendix A.

Figure 2. Transmitter microphone coupled to the ear simulator

5. CONSIDERATIONS FOR THE TIME DOMAIN TRANSFORMATION

Returning to the issue of determining the impulse response, it was shown in Section 3 that an inverse Fourier transform (IFT) needs to be applied. A brief review of this operation can be found in Appendix B. An important point to note is that the definition of the IFFT indicates that it operates on a frequency range extending to infinity. In practice this means finding an upper frequency beyond which the system response become insignificant.

A further issue arising from computation requirements is that of the number of steps needed in the stepped-sine frequency response. First these steps need to be linearly spaced, and second the number of steps and the upper frequency limit together define the step size that is used. The step size in turn dictates the resolution and overall duration that can be obtained in the time domain following the transformation.

These issues have been carefully considered in developing the test method. At first, an estimated upper frequency of 30 kHz was thought to be acceptable, based on the rapid attenuation in the ear simulator response above 20 kHz, indicated by the lumped parameter model. However, initial results caused this parameter to be revised and an upper frequency of 100 kHz, the limit of the 2-channel analyser, was eventually used. The 2-channel analyser was capable of measuring a maximum of 10,000 points in a frequency response. The speed at which the system operates enabled this maximum number of points to be used. This provided the best possible time-domain resolution with a run time of only 15 minutes.

6. EXPERIMENTAL RESULTS

Initial measurements made with the system extended to 30 kHz, but surprisingly the high frequency response obtained did not tend towards zero as might be predicted from the expected dynamic response of the microphones. This prompted further investigations leading to the result shown in Fig. 3. Note that this result is not a full implementation of Eq. 5; it is experimental data of the voltage ratio. However it does illustrate that there remains significant energy above 20 kHz.

Most likely, this response is caused by acoustic resonances within the primary cavity, the secondary volumes being effectively blocked by the coupling tubes and slots at these frequencies. However the transmitter microphone was thought to have insufficient sensitivity at these frequencies to enable high-order modes to be generated. An alternative explanation was that the observed response could be due to electrical disturbance such as cross-talk.

This primary cavity has the shape of a truncated cone, or frustum, so predicting the frequencies associated with resonances in cavity of this shape to validate this assumption, is not straight-forward.

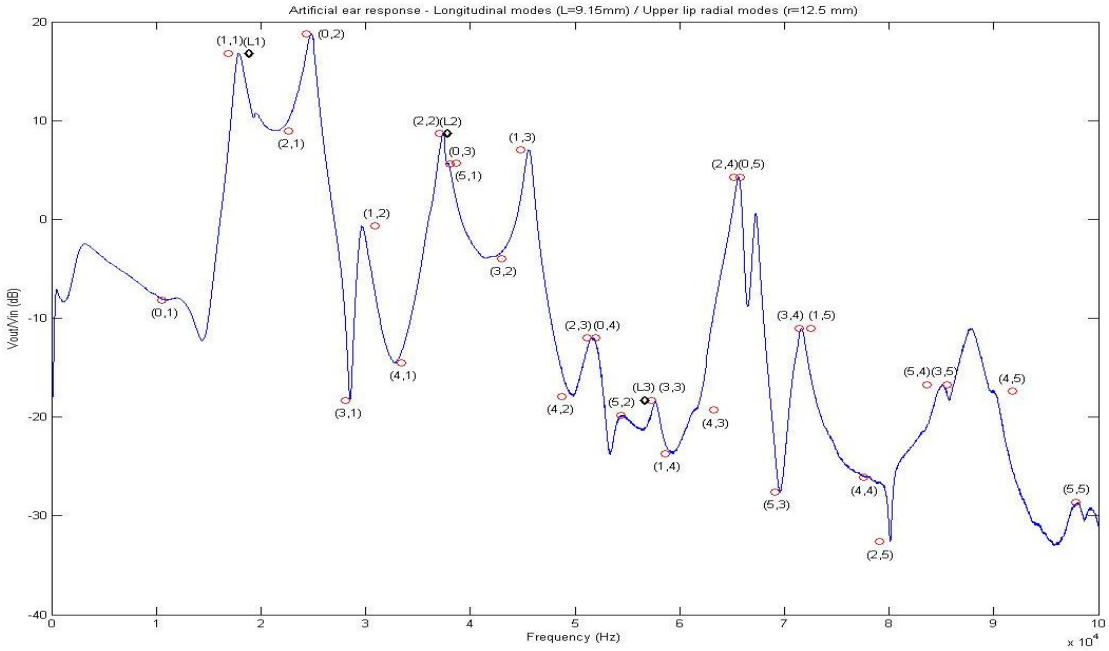

Figure 3. Frequency response of the artificial ear up to 100 kHz

Appendix C develops the theory leading to an estimate of the radial and longitudinal modes expected in this frequency range. These are also indicated in Fig. 3. The longitudinal modes are indicated by L1, L2 and L3 and the circular modes by 2 figures in parenthesis. The first figure denotes the order of radial modes and the second the order of diametric modes (see Appendix C). The calculations were performed under reference environmental conditions (23 ºC, 101.325 kPa and 50% relative humidity) rather than the conditions during the particular measurement. In addition there is some uncertainty in the actual dimensions of the cavity, partly due

to manufacturing tolerances and partly due to the exact location of the microphone within the structure. Both these factors mean that the observed peaks in the response should not necessarily coincide exactly with the calculated resonance frequencies, but the calculated values provide a qualitative indication of where these peaks should lie.

Although some of the calculated resonance frequencies do not appear to correspond with peaks in the response, every peak can be associated with a particular resonant mode. It therefore seems that the measured response is indeed due to acoustical resonance within the cavity. Consequently, all further measurements were conducted up to 100 kHz, the full frequency range capability of the instrumentation.

The extended frequency range also meant that additional data on the transmitter microphone sensitivity was required. Acoustical calibration methods are not possible above 25 kHz, so an electrostatic actuator response was used. Fig. 4 shows the results of these measurements for the transmitter microphone. The response of the microphone up to 50 kHz was as expected from existing knowledge. However no published data exists for the frequency range beyond this. The peaks in the response observed between 50 kHz and 100 kHz could be the result of resonances in the microphone diaphragm or back cavity, in which case they are valid for our measurement, or they could be a result of interaction between the microphone and actuator, and therefore not relevant when the microphone is actually used. Certainly the peak at 60 kHz can be linked to a length resonance in the back cavity of the microphone, suggesting that the structure seen in this region results from the microphone response.

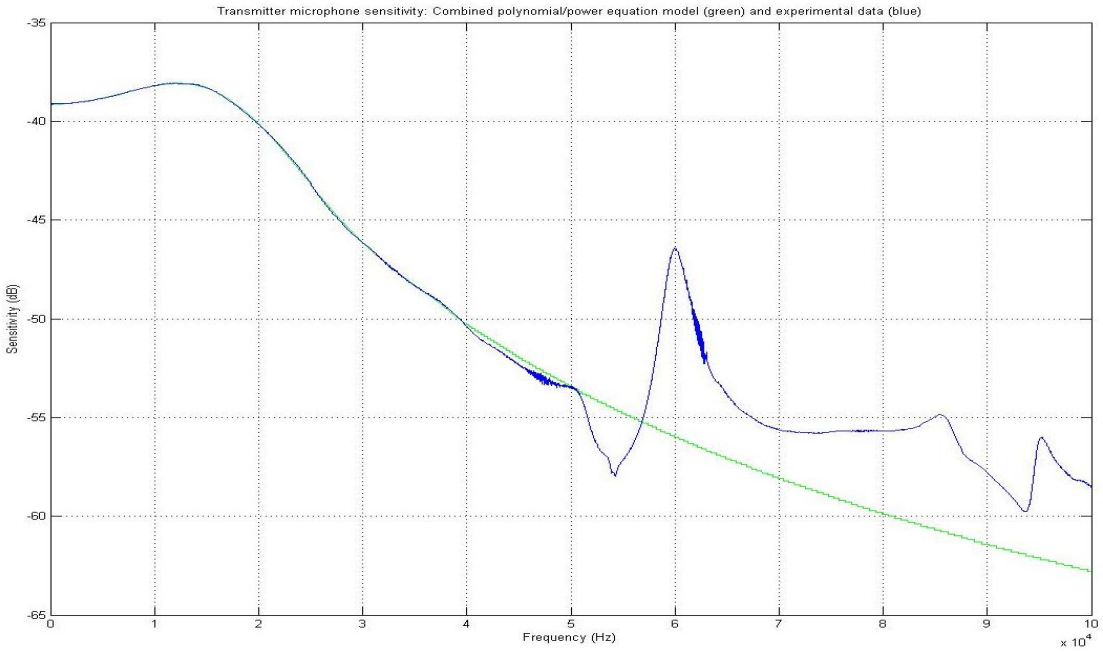

Figure 4. Electrostatic actuator response of the transmitter microphone (Brüel & Kjær type 4134), fitted with a polynomial function

Given the uncertainty in the origin of some elements of the microphone response, two approaches were adopted for including the transmitter microphone sensitivity in the volume velocity sensitivity calculation. The first approach was to simply take the

measurement data (Approach 1), and the second approach to fit polynomial functions in the reliable part of the frequency range and extrapolate this to 100 kHz (Approach 2). The result of the fitting is shown in Fig. 4. The difference arising from using these two approaches in the final calculation of the impulse response will be examined below.

The final element of Eq. 5 to be determined is the value of the capacitor used to measure the input current applied to the transmitter microphone. This has been measured and its value found to change less than 1% over the frequency range of interest. A value of 95.3 nF was therefore used throughout.

Implementing Eq. 5 therefore leads to the volume velocity frequency response shown in Fig. 5, and following transformation into the time domain, the impulse response shown in Fig. 6.

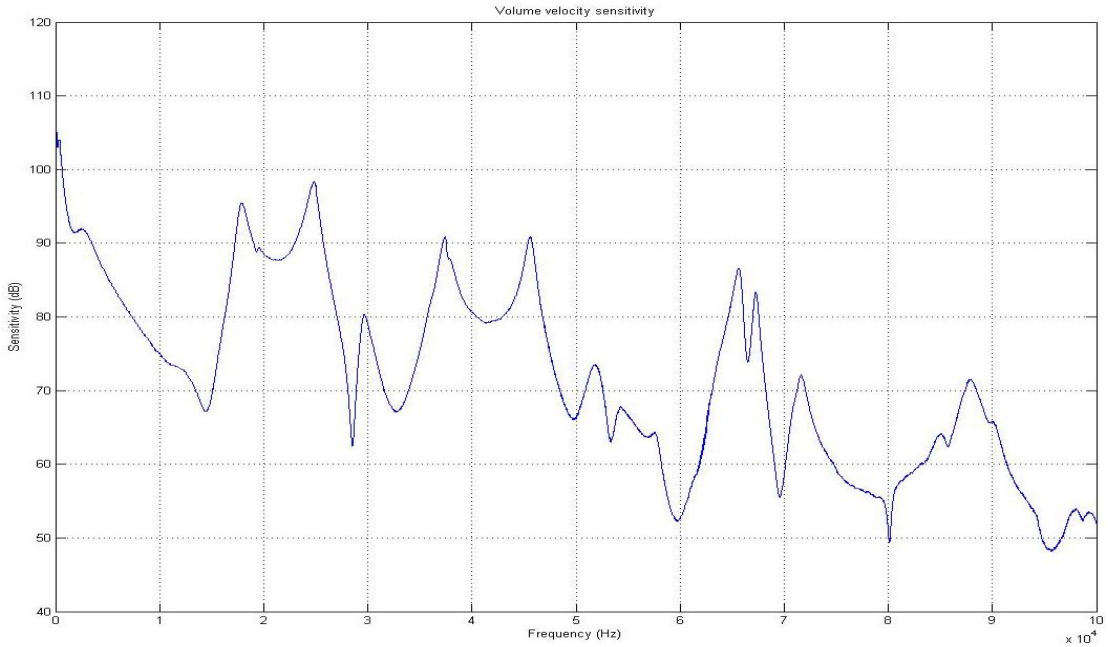

Figure 5. Volume velocity sensitivity as a function of frequency

Impulse response is characterised by a single number given by the peak value reached at the start of the time response. The impulsive volume velocity sensitivity can then be compared directly with steady-state values at a specific frequency simply by extracting this steady-state value from the frequency response data.

For the data shown in Fig. 6, this peak value is 80.68 dB re. 1V / m^3s^{-1}.

IEC 60645-3 recommends a reference frequency of 1 kHz for evaluating the equivalent peak-to-peak sound pressure. The corresponding volume velocity sensitivity at this frequency is 95.40 dB re 1V / m^3s^{-1}. Since the volume velocity sensitivity is directly proportional to the impedance, large variations with frequency are to be expected, especially at low frequencies.

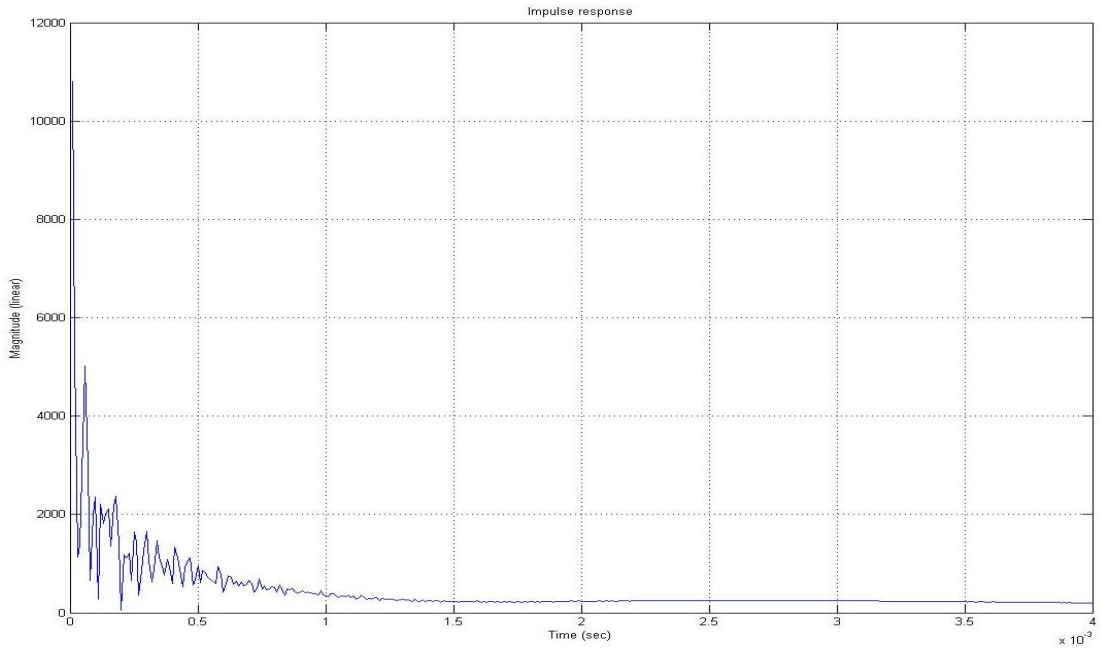

Figure 6. Impulse response (first 4 ms) generated from the data shown in Fig. 5

Before going on to consider how these results impact on the current IEC recommendations, it is interesting to consider how the response of a particular transmitter might affect the situation.

The results for the impulse response quoted above only remain valid if the input stimulus contains energy over the full frequency range. This is unlikely, so to estimate the effect of a limited bandwidth source, it is possible to use the same input data but progressively reduce the upper frequency limit of the data that is processed. Table 1 shows the change in results for different upper cut-off frequencies.

Upper frequency limit (kHz)	Volume velocity sensitivity from impulse response (dB 1V / m^3s^{-1})	Volume velocity sensitivity at 1 kHz (dB 1V / m^3s^{-1})	Difference (dB)
100	80.68	95.40	14.72
50	85.73	95.40	9.67
20	87.57	95.40	7.83
10	90.17	95.40	5.23
5	94.70	95.40	0.70

Table 1: Comparison between the steady-state response at 1 kHz and the impulse response determined with different frequency ranges

The general conclusion to be drawn from these results is that the greater the bandwidth of the transducer (which is a general indicator of the quality of the device), the greater the error will be if the sensitivity of the artificial ear is taken to be that at 1 kHz.

The other issue remaining from earlier within this report is what data to use for the microphone sensitivity, particularly above 50 kHz. Using the same data illustrated in

Fig. 4, and applying to two options for the microphone sensitivity in Eq. 5, results in values for the transient volume velocity sensitivity of 80.68 dB if the measured data is used and 80.99 dB if the microphone sensitivity derived from the polynomial expression is used. These values are sufficiently close to conclude that the transient volume velocity sensitivity is not strongly dependent on the microphone response above 50 kHz, and that it does not matter which approach is used. If the data is limited to the range up to 50 kHz, differences reduce to less than 0.05 dB.

7. CONCLUSIONS

For a transducer driven sinusoidally at a particular frequency, the sound pressure developed within the artificial ear is directly proportional to the acoustical impedance at that frequency, and can be measured with a calibrated microphone. When the transducer is driven impulsively, it still drives the artificial ear with a volume velocity, but there is now no associated frequency and the corresponding value of the acoustical impedance is unclear, since it is strongly frequency dependent.

The practice that is currently adopted is to specify a reference frequency of 1 kHz, and perform an equivalent peak-to-peak steady-state measurement of the transient signal. This implicitly assumes that the equivalent effective impedance under transient conditions is the same as that at 1 kHz, but there has been no evidence for this. Where different frequencies are selected for performing the equivalent peak-to-peak measurement, very different values can be obtained for the calculated sound pressure. For example if 250 Hz were used instead of 1 kHz, the value would be 9 dB higher.

In this report the impulse response was used as the basis for specifying the sensitivity of the artificial ear for the measurement of transient signals. This has been derived from steady-state measurements of the volume velocity sensitivity as a function of frequency, and applying an inverse Fourier transform. The results obtained show that there is a difference of 14.72 dB between the calculated impulse response, and the steady-state sensitivity at 1 kHz, which translates directly as a difference in the sound pressure derived from the artificial ear measurement. If the ‘equivalent peak-to-peak’ approach is maintained, these measurements show that a reference frequency of approximately 4 kHz (precisely 4.4 kHz in the example of the artificial ear used for these measurements, but manufacturing tolerances mean that other examples should require the same tolerance frequency) minimises the difference between the two responses.

The new information presented in this report leads to a number of possible outcomes.

(a) Current practice can remain the same, but with the added information about the level of difference between the estimated and likely actual sound pressure level generated by the earphone.

(b) The reference frequency specified in future revisions of IEC 60645-3 could be reset to a value where the impulse and steady-state response of a typical ear simulator was the same (estimated to be 4.4 kHz), but the tolerance in impedance of a range of ear simulators needs also to be taken into account.

(c) Individual ear simulators could be calibrated in terms of their impulse response, by the method described in this report. The resulting sensitivity can then be used to estimate the output of all transducers.

(d) The approach in (c) can be extended by considering the actual time domain response of the stimulus applied to the transducer in audiometric testing, and performing a convolution of this with the measurement impulse response to produce the sound pressure generated by the particular stimulus. This approach has the widest potential application as it can be used with test stimuli that do not

have the idealised forms specified by IEC. It can also take account of any distortion of the applied waveform by the transducer.

8. REFERENCES

[1] BS EN 60645-1:2001, “Audiological Equipment - Part 1: Pure-tone audiometers”.

[2] IEC 60318-1:1998, “Electroacoustics - Simulators of human head and ear - Part 1: Ear simulator for the calibration of supra-aural earphones”.

[3] IEC 60711:1981, “Occluded-ear simulator for the measurement of earphones coupled to the ear by ear inserts”.

[4] IEC 60645-3: 2006, “Electroacoustics – audiometric equipment, Part 3: test signals of short duration”.

[5] D.R. Jarvis, “Realisation of the standard of sound pressure through the calibration of half-inch laboratory standard condenser microphones”, PhD thesis, University of London, Kings College, 1989.

APPENDIX A - LIST OF EQUIPMENT

The measurement system consisted of the following equipment

Brüel & Kjær Pulse system INCL. Noise Generator	
H&H power amplifier	Type TPA 50·D
Transmitter section (in house construction)	
Brüel & Kjær WS2 microphone (Transmitter)	Type 4134
Brüel & Kjær adaptor 1" to ½"	
Brüel & Kjær Coupler adaptor ½" to 1"	DB 0025
Brüel & Kjær Coupler adaptor	DB 3977
Brüel & Kjær artificial ear (coupler)	Type 4153
Brüel & Kjær WS2 microphone (Receiver)	Type 4134
Norsonic. Preamplifier	Type 1201
Vinculum microphone power unit (Transmitter)	Type E711
Vinculum microphone power unit (Receiver)	Type E711
Measurement capacitor (in house construction)	

For measurements using a half-inch transmitter, the microphone grid was removed and the microphone was fitted with an adaptor type DB 0025 to enable fitting into the coupler adaptor type DB 3977.

APPENDIX B - INVERSE FOURIER TRANSFORM

As discussed in the main body of the report, the impulse response of the system can be obtained, as discussed, by applying a suitable Inverse Fourier Transform (IFT) on the frequency response of the volume velocity sensitivity.

The Fourier Transform (FT) and Inverse Fourier Transform (IFT) integrals are given by[6],

$$F(j\omega) = \int_{-\infty}^{\infty} f(t) e^{-j\omega t} dt \qquad \textbf{(B1)}$$

$$f(t) = \frac{1}{2\pi} \int_{-\infty}^{\infty} F(j\omega) e^{j\omega t} d\omega \qquad \textbf{(B2)}$$

where $f(t)$ is a time domain function.

Because time-domain functions generally consist of continuous data, the numerical realisation of the FT and IFT integrals is difficult. For this reason, a signal must be sampled and treated as a numeric sequence.

The Fourier and Inverse Fourier Transforms are then modified to produce the Discrete Fourier Transform (DFT) and Inverse Discrete Fourier Transform (IDFT) which are given by,

$$F(k) = \sum_{n=0}^{N-1} f(n) e^{-\frac{2\pi i}{N} kn} \qquad \textbf{(B3)}$$

$$f(n) = \frac{1}{N} \sum_{n=0}^{N-1} F(k) e^{\frac{2\pi i}{N} kn} \qquad \textbf{(B4)}$$

where $f(n)$ is the digitised version of $f(t)$.

To improve computational efficiency, the DFT and IDFT are modified to produce the Fast Fourier Transform (FFT) and Inverse Fast Fourier Transform (IFFT) respectively, which are used in signal processing packages, digital units and applications.

The close relationship between the data in the frequency and time domains means that parameters in one domain dictate corresponding parameters in the other. For instance, a system utilising 10,000 samples (n) and with upper frequency limit of 20 kHz (f_T),

would produce a time window of,

$$\Delta f = \frac{f_T}{n} = 2 \text{ Hz}$$

$$\Delta t = \frac{1}{n\Delta f} = 50 \times 10^{-6} \text{ s}$$

$$t_T = n\Delta t = 0.5 \text{ s}$$

while a system utilising 10,000 samples and with upper frequency limit of 100 kHz, would produce a maximum time window of,

$$\Delta f = \frac{f_T}{n} = 10 \text{ Hz}$$

$$\Delta t = \frac{1}{n\Delta f} = 10 \times 10^{-6} \text{ s}$$

$$t_T = n\Delta t = 0.1 \text{ s}$$

By extending the measurement frequency range to include higher frequencies, one is able to produce (through an IFFT) an impulse response that contains more information as opposed to an impulse response that resulted from a limited measurement frequency range. In other words, the latter would appear smoother in shape as opposed to the former.

[6] E.C. Ifeachor, B.W. Jervis, “Digital signal processing – a practical approach”, Addison-Wesley Ltd., USA, 1996.

APPENDIX C - DETERMINATION OF LONGITUDINAL AND RADIAL MODES IN WAVEGUIDES

The theory used to identify the frequencies at which longitudinal and radial modes develop in a cylindrical waveguide can be also applied to conical and conical frustum waveguides with some modifications regarding their physical dimensions[7].

In cylindrical waveguides, the equation that predicts the frequencies of longitudinal modes is given by,

$$f_n = \frac{nc}{2L} \qquad \textbf{(C1)}$$

where n is the harmonic number
c is the speed of sound
L is the physical length of the waveguide

while the equation that predicts the frequencies of radial modes is given by,

$$f_{mn} = \frac{j_{mn}c}{2\pi r} \qquad \textbf{(C2)}$$

where j_{mn} are the coefficients representing the zeros of the Bessel functions of the first kind, c is the speed of sound and r is the radius of the cylinder.

The j_{mn} coefficients required to calculate radial modes (0,1) to (5,5) are shown in the following table.

n / **m**	**0**	**1**	**2**	**3**	**4**	**5**
0	-	2.40	5.52	8.65	11.79	14.93
1	0	3.83	7.02	10.17	13.32	16.47
2	0	5.14	8.42	11.62	14.80	17.96
3	0	6.38	9.76	13.02	16.22	19.41
4	0	7.59	11.06	14.37	17.62	20.83
5	0	8.77	12.34	15.70	18.98	22.22

Table C1: Zeros - Bessel functions of the first kind

The radial modes of a circular membrane may be seen in Figure C1[8]. The hatched and un-hatched sections denote areas that move out-of-phase with respect to each other.

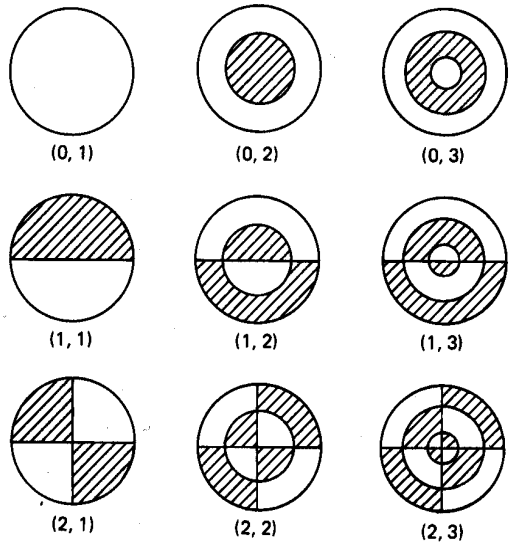

Figure C1: Normal modes of a circular membrane

Successive orders of longitudinal modes given by *n* in Eq. C1 form a harmonic series.

This is not quite the case for the radial modes, where the frequency of each is governed by the factor j_{mn}. There are two types of radial modes to consider, therefore by arranging these coefficients in ascending order, it is possible to predict the order of appearance of the radial modes. This is shown in Table C2. Notice that they do not form a harmonic series. However ordering is very helpful in identifying particular radial modes in a frequency response.

A cylindrical waveguide is characterised by a single radius along its length. However, if the waveguide radius changes linearly along its length, the resulting shape is called a frustum. Fig. C2 presents a cylindrical and a frustum waveguide with their dimensions.

The longitudinal and radial modes developed in a frustum waveguide are also given by Eqs. C1 and C2, but with some modifications to the interpretation of the geomtrical paramneters. The length parameter in Eq. C1 represents the length of the side of the frustum L_{fr}[7]. The radius in Eq. C2 represents the upper lip of the frustum.

The speed of sound is also important for calculating resonance frequencies. This depends on environmental conditions[9], particularly the temperature, and these dependencies need to be accounted for. However, at 23°C, 50% humidity and a pressure of 1013.25 mbar, the value for c is 345.9 ms^{-1}.

Order	Radial mode	Order	Radial mode
1	*0,1*	16	*5,2*
2	*1,1*	17	*3,3*
3	*2,1*	18	*1,4*
4	*0,2*	19	*4,3*
5	*3,1*	20	*2,4*
6	*1,2*	21	*0,5*
7	*4,1*	22	*5,3*
8	*2,2*	23	*3,4*
9	*0,3*	24	*1,5*
10	*5,1*	25	*4,4*
11	*3,2*	26	*2,5*
12	*1,3*	27	*5,4*
13	*4,2*	28	*3,5*
14	*2,3*	29	*4,5*
15	*0,4*	30	*5,5*

Table C2: Order of appearance of radial modes in a circular membrane

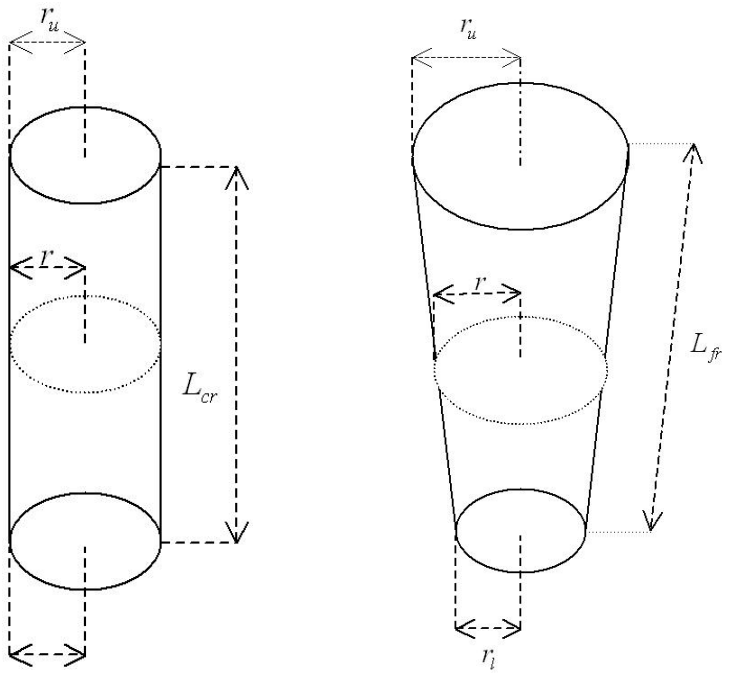

Figure C2: A cylindrical and a frustum waveguide

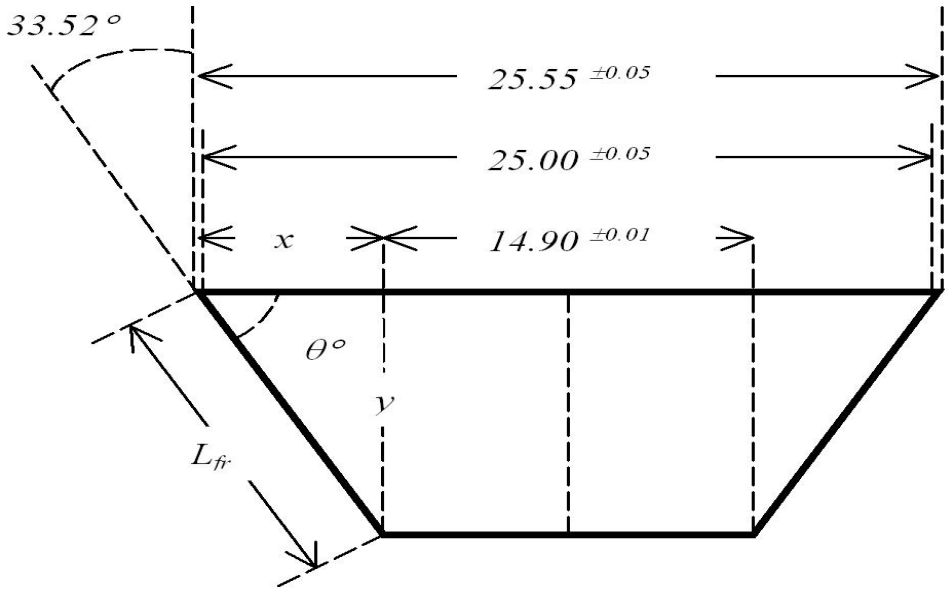

Figure C3: Geometry of the artificial ear waveguide (dimensions in mm)

Fig. C3 shows the actual geometry of the artificial ear.

The transmitter and receiver microphones were placed on the *upper lip* and throat respectively of the artificial ear. Appendix A provides the mathematical basis that describes and calculates the particular frequencies at which longitudinal and radial modes will appear.

The length (L_{fr}) of the side of this particular conical frustum needs to be calculated first:

$$\theta = 90° - 33.52° = 56.48°$$

$$x = \frac{25.00}{2} - \frac{14.90}{2} = 12.50 - 7.45 = 5.05 \text{ mm}$$

$$\cos(\theta) = \frac{x}{L_{fr}} \quad \Rightarrow \quad L_{fr} = \frac{x}{\cos(\theta)} = \frac{5.05}{\cos(56.48)} = 9.15 \text{ mm}$$

$$L_{fr} = 9.15 \text{ mm}$$

Tables C3 and C4 give the resonance frequency calculated for this geometry.

Harmonic (n)	**F_{th} (Hz)**
1	18902
2	37803
3	56705

Table C3: The theoretical frequencies for the longitudinal modes of the artificial ear

Radial mode	**F_{th} (Hz)**
0,1	10570
1,1	16868
2,1	22637
0,2	24311
3,1	28098
1,2	30917
4,1	33427
2,2	37083
0,3	38096
5,1	38624
3,2	42984
1,3	44790
4,2	48710
2,3	51176
0,4	51925
5,2	54347
3,3	57342
1,4	58663
4,3	63287
2,4	65181
0,5	65754
5,3	69145
3,4	71435
1,5	72536
4,4	77601
2,5	79098
5,4	83591
3,5	85484
4,5	91738
5,5	97860

Table C4: The theoretical frequencies for the radial modes of the artificial ear

[7] R.D. Ayers, L. J. Eliason, D. Mahgerefteh, “The conical bore in musical acoustics”, American Journal of Physics, Vol 53, No. 6, pp 528-537, June 1985.

[8] L.E. Kinsler, A.R. Frey, A.B. Coppens, J.V. Sanders, “Fundamentals of Acoustics”, Fourth Edition, John Wiley & Sons Inc., USA, 2000.

[9] O. Cramer, “The variation of the specific heat ratio and the speed of sound in air with temperature, pressure, humidity and CO_2 concentration”, Journal of the Acoustical Society of America, 93 (5), pp 2510-2516, May 1993.